J|A|C|S
ARTICLES

Published on Web 10/25/2008

Simple and Generalized Synthesis of Oxide−Metal Heterostructured Nanoparticles and their Applications in Multimodal Biomedical Probes

Sang-Hyun Choi,† Hyon Bin Na,† Yong Il Park,† Kwangjin An,† Soon Gu Kwon,† Youngjin Jang,† Mi-hyun Park,† Jaewon Moon,† Jae Sung Son,† In Chan Song,‡ Woo Kyung Moon,‡ and Taeghwan Hyeon*,†

National Creative Research Initiative Center for Oxide Nanocrystalline Materials and School of Chemical and Biological Engineering, Seoul National University, Seoul 151-744, Korea, and Department of Radiology, Seoul National University College of Medicine, Seoul National University Hospital, Seoul 110-744, Korea

Received July 9, 2008; E-mail: thyeon@snu.ac.kr

Abstract: Heterostructured nanoparticles composed of metals and Fe_3O_4 or MnO were synthesized by thermal decomposition of mixtures of metal−oleate complexes (for the oxide component) and metal−oleylamine complexes (for the metal component). The products included flowerlike-shaped nanoparticles of Pt−Fe_3O_4 and Ni−Fe_3O_4 and snowmanlike-shaped nanoparticles of Ag−MnO and Au−MnO. Powder X-ray diffraction patterns showed that these nanoparticles were composed of face-centered cubic (fcc)-structured Fe_3O_4 or MnO and fcc-structured metals. The relaxivity values of the Au−MnO and Au−Fe_3O_4 nanoparticles were similar to those of the MnO and Fe_3O_4 nanoparticles, respectively. Au−Fe_3O_4 heterostructured nanoparticles conjugated with two kinds of 12-base oligonucleotide sequences were able to sense a complementary 24-mer sequence, causing nanoparticle aggregation. This hybridization-mediated aggregation was detected by the overall size increase indicated by dynamic light scattering data, the red shift of the surface plasmon band of the Au component, and the enhancement of the signal intensity of the Fe_3O_4 component in T_2-weighted magnetic resonance imaging.

Introduction

Colloidal nanoparticles have been extensively utilized in various technological areas because of their unique size-dependent electronic, optical, and magnetic properties.[1] In particular, different kinds of nanoparticles have been extensively used in biomedical applications.[2] For example, various magnetic nanoparticles have been used as magnetic resonance imaging (MRI) contrast agents, magnetic drug-delivery vehicles, and in bioseparations.[3] Our group recently developed a new T_1 MRI contrast agent using MnO nanoparticles.[4] Semiconductor nanoparticles have been used as fluorescent probes for cell labeling, tracking, and imaging.[5] Au nanoparticles derivatized with oligonucleotides can sense complementary DNA (cDNA) strands, as detected by color changes resulting from the shift of surface plasmon resonance peaks between isolated and aggregated nanoparticles.[6] Recently, various heterostructured nanoparticles composed of two different kinds of materials have been synthesized,[7] merging the properties of the individual materials and creating the potential for new multifunctional biomedical applications. For example, Sun and co-workers synthesized heterostructured nanoparticles composed of ferrite and Au[8a] or Ag[8b] and used them as a dual MRI and optical-imaging probe[8c] in a magneto-optical application,[8b] respectively. However, most of the reported syntheses of heterostructured

† School of Chemical and Biological Engineering, Seoul National University.

‡ Department of Radiology, Seoul National University College of Medicine.

(1) (a) *Nanoscale Materials in Chemistry*; Klabunde, K. J., Ed.; Wiley-Interscience: New York, 2001. (b) *Nanoparticles and Nanostructured Films*; Fendler, J. H., Ed.; Wiley-VCH: Weinheim, Germany, 1998. (c) Alivisatos, A. P. *Science* **1996**, *271*, 933–937. (d) Hyeon, T. *Chem. Commun.* **2003**, 927–934. (e) Park, J.; Joo, J.; Kwon, S. G.; Jang, Y.; Hyeon, T. *Angew. Chem., Int. Ed.* **2007**, *46*, 4630–4660.

(2) (a) Niemeyer, C. M.; Mirkin, C. A. *Nanobiotechnology: Concepts, Applications and Perspectives*; Wiley-VCH: Weinheim, Germany, 2004. (b) Wang, J. *Small* **2005**, *1*, 1036–1043.

(3) (a) Weissleder, R.; Kelly, K.; Sun, E. Y.; Shtatland, T.; Josephson, L. *Nat. Biotechnol.* **2005**, *23*, 1418–1423. (b) Bulte, J. W. M.; Zhang, S. C.; Van Gelderen, P.; Herynek, V.; Jordan, E. K.; Duncan, I. D.; Frank, J. A. *Proc. Natl. Acad. Sci. U.S.A.* **1999**, *96*, 15256–15261. (c) Jun, Y. W.; Huh, Y. M.; Choi, J. S.; Lee, J. H.; Song, H. T.; Kim, S.; Yoon, S.; Kim, K. S.; Shin, J. S.; Suh, J. S.; Cheon, J. *J. Am. Chem. Soc.* **2005**, *127*, 5732–5733. (d) Gu, H.; Ho, P. L.; Tsang, K. W. T.; Wang, L.; Xu, B. *J. Am. Chem. Soc.* **2003**, *125*, 15702–15703. (e) Xu, C.; Xu, K.; Gu, H.; Zhong, X.; Guo, Z.; Zheng, R.; Zhang, X.; Xu, B. *J. Am. Chem. Soc.* **2004**, *126*, 3392–3393. (f) Xu, C.; Xu, K.; Gu, H.; Zheng, R.; Liu, H.; Zhang, X.; Guo, Z.; Xu, B. *J. Am. Chem. Soc.* **2004**, *126*, 9938–9939.

(4) Na, H. B.; Lee, J. H.; An, K.; Park, Y. I.; Park, M.; Lee, I. S.; Nam, D.-H.; Kim, S. T.; Kim, S.-H.; Kim, S.-W.; Lim, K.-H.; Kim, K.-S.; Kim, S.-O.; Hyeon, T. *Angew. Chem., Int. Ed.* **2007**, *46*, 5397–5401.

(5) (a) Dubertret, B.; Skourides, P.; Norris, D. J.; Noireaux, V.; Brivanlou, A. H.; Libchaber, A. *Science* **2002**, *298*, 1759–1762. (b) Medintz, I. L.; Uyeda, H. T.; Goldman, E. R.; Mattoussi, H. *Nat. Mater.* **2005**, *4*, 435–446. (c) Michalet, X.; Pinaud, F. F.; Bentolila, L. A.; Tsay, J. M.; Doose, S.; Li, J. J.; Sundaresan, G.; Wu, A. M.; Gambhir, S. S.; Weiss, S. *Science* **2005**, *307*, 538–544. (d) Klostranec, J. M.; Chan, W. C. W. *Adv. Mater.* **2006**, *18*, 1953–1964.

(6) (a) Taton, T. A.; Mirkin, C. A.; Letsinger, R. L. *Science* **2000**, *289*, 1757–1760. (b) Nam, J. M.; Thaxton, C. S.; Mirkin, C. A. *Science* **2003**, *301*, 1884–1886.

 © 2008 American Chemical Society

nanoparticles have involved expensive, toxic reagents and complicated multistep syntheses. We herein report the syntheses of various heterostructured metal−oxide nanoparticles composed of a metal (Au, Ag, Pt, or Ni) and a metal oxide (Fe_3O_4 or MnO) through simple thermal decomposition of metal−surfactant complexes derived from inexpensive, nontoxic metal salts.

Experimental Section

Heterostructured Ni−Fe_3O_4 Nanoparticles. An Fe−oleate complex was synthesized by a previously reported method.[9a] A 0.90 g sample of the Fe−oleate complex (1 mmol) was dissolved in 10 mL of 1-octadecene and 1.30 g of 1,2-hexadecanediol at room temperature and heated to 100 °C in a vacuum, forming a homogeneous, clear, brown solution. A Ni−oleylamine complex solution was prepared by mixing 1 mL of oleylamine, 25 mg of nickel(II) chloride hydrate (0.05 mmol), and 5 mL of 1-octadecene followed by sonication for 30 min. The Ni−oleylamine complex solution was injected into the Fe−oleate complex solution at 140 °C, and the resulting mixture was annealed at that temperature for 20 min, subsequently heated to 230 °C, and aged at that temperature for 30 min, resulting in a deep-green colloidal solution. The precipitate of Ni−Fe_3O_4 nanoparticles was generated by addition of 20 mL of ethanol and 20 mL of acetone and isolated by centrifugation, producing a brown product that was dispersible in many organic solvents, such as toluene, hexane, and octane. The same isolation process was used in the remaining synthetic schemes.

Heterostructured Au−Fe_3O_4 Nanoparticles. An Fe−oleate complex solution was produced as described above. A Au−oleylamine complex solution was prepared by mixing 1 mL of oleylamine, 40 mg of hydrogen tetrachloroaurate(III) hydrate (0.1 mmol), and 5 mL of 1-octadecene followed by sonication for 30 min. The Au−oleylamine complex solution was injected into the Fe−oleate complex solution at 140 °C, and the resulting mixture was annealed at that temperature for 20 min, subsequently heated to 230 °C, and aged at that temperature for 30 min, resulting in a violet colloidal solution.

Heterostructured Au−MnO Nanoparticles. A Mn−oleate complex was synthesized by a previously reported method.[9a] A 1.24 g sample of the Mn−oleate complex (2 mmol) was dissolved in 10 mL of 1-octadecene and 1.30 g of 1,2-hexadecanediol at room temperature and heated to 100 °C under vacuum, forming a homogeneous, clear, brown solution. A Au−oleylamine complex solution was prepared in advance as described above and injected into the Mn−oleate complex solution at 140 °C. After the injection, the solution was aged at 140 °C for 20 min, heated to 300 °C, and annealed at that temperature for 40 min, resulting in a violet colloidal solution.

Heterostructured Ag−MnO Nanoparticles. A 0.62 g sample of the Mn−oleate complex (1 mmol) was dissolved in 10 mL of 1-octadecene and 1.30 g of 1,2-hexadecanediol at room temperature and heated to 100 °C under vacuum, forming a clear brown solution. A Ag−oleylamine complex solution, which had been prepared by mixing 1 mL of oleylamine, 14.3 mg of silver nitrate (0.1 mmol), and 5 mL of 1-octadecene followed by sonication for 30 min, was injected into the Mn−oleate complex solution at 140 °C, after which the mixture was annealed for 20 min, heated to 300 °C, and aged at that temperature for 30 min, resulting in a brown colloidal solution.

Heterostructured Pt−Fe_3O_4 Nanoparticles. An Fe−oleate complex solution was prepared as described above. A Pt−oleylamine complex solution, which had been prepared by mixing 1 mL of oleylamine, 25.8 mg of tetrachloroplatinate(III) hydrate (0.05 mmol), and 5 mL of 1-octadecene followed by 30 min sonication, was injected into the Fe−oleate complex solution at 140 °C. The resulting mixture was annealed for 20 min and then heated to 300 °C for 30 min, yielding a black colloidal solution.

Characterization. The heterostructured nanoparticles were characterized by transmission electron microscopy (TEM), electron diffraction (ED), and X-ray diffraction (XRD). The size distribution and crystallinity of the nanoparticles were examined by TEM using a JEOL JEM-2010 microscope operating at 200 kV. Powder XRD of the nanoparticles was performed using a Rigaku D/Max-3C diffractometer with Cu Kα radiation ($\lambda = 0.15418$ nm). The magnetic properties of the Pt−Fe_3O_4 nanoparticles were characterized using a superconducting quantum interference device (SQUID, Quantum Design MPMS 5XL magnetometer) over the temperature range 5−300 K.

Water-Dispersed Heterostructured Nanoparticles of Au−MnO and Au−Fe_3O_4. Water-dispersed nanoparticles of Au−MnO and Au−Fe_3O_4 were prepared via the method published previously,[5a] with some modifications involving encapsulation of the nanoparticles dispersed in chloroform with 1,2-distearoyl-*sn*-glycero-3-phosphoethanolamine-*N*-[methoxy(polyethylene glycol)-2000] (mPEG-2000 PE, Avanti Polar Lipids, Inc.). Typically, 3 mL of Au−MnO or Au−Fe_3O_4 nanoparticles in chloroform (5 mg/mL) was mixed with 1 mL of chloroform containing 30 mg of mPEG-2000 PE. After evaporation of the solvent, the remaining material was incubated at 70 °C under vacuum for 1 h, and then 5 mL of water was added. The resulting suspension was filtered, and excess PEG−phospholipid starting material was removed by ultracentrifugation.

Measurement of MRI Properties of the Nanoparticles. A 1.5 T clinical MRI scanner was used to measure the T_1 and T_2 relaxation times for various concentrations of the nanoparticles dispersed in water. An IR-FSE sequence with 30 different values of T_I ($T_R/T_E/T_I$ = 4400 ms/13 ms/24−4000 ms) for T_1 measurements and a conventional CPMG sequence with 12 different T_E values (T_R/T_E = 3300 ms/13, 26, 39, 52, 70, 140, 210, 280, 400, 800, 1200, and 1600 ms) for T_2 measurements were performed with a head coil on the 1.5 T MRI scanner. T_1 and T_2 relaxation times were calculated by fitting the signal intensities with increasing T_E or T_I to a monoexponential function of the form $|[1 - (1 - k)\exp(-T_I/$

(7) (a) Cozzoli, P. D.; Pellegrino, T.; Manna, L. *Chem. Soc. Rev.* **2006**, *35*, 1195–1208. (b) Mokari, T.; Sztrum, C. G.; Salant, A.; Rabani, E.; Banin, U. *Nat. Mater.* **2005**, *4*, 855–863. (c) Mokari, T.; Rothenberg, E.; Popov, I.; Costi, R.; Banin, U. *Science* **2004**, *304*, 1787–1790. (d) Teranishi, T.; Inoue, Y.; Nakaya, M.; Oumi, Y.; Sano, T. *J. Am. Chem. Soc.* **2004**, *126*, 9914–9915. (e) Gu, H.; Zheng, R.; Zhang, X.; Xu, B. *J. Am. Chem. Soc.* **2004**, *126*, 5664–5665. (f) Kim, H.; Achermann, M.; Balet, L.; Hollingsworth, J. A.; Klimov, V. J. *J. Am. Chem. Soc.* **2005**, *127*, 544–546. (g) Kwon, K.-W.; Shim, M. *J. Am. Chem. Soc.* **2005**, *127*, 10269–10275. (h) Kudera, S.; Carbone, L.; Casula, M. F.; Cingolani, R.; Falqui, A.; Snoeck, E.; Parak, W. J.; Manna, L. *Nano Lett.* **2005**, *5*, 445–449. (i) Gu, H.; Zheng, R.; Liu, H.; Zhang, X.; Xu, B. *Small* **2005**, *1*, 402–406. (j) Gu, H.; Yang, Z.; Gao, J.; Chang, C. K.; Xu, B. *J. Am. Chem. Soc.* **2005**, *127*, 34–35. (k) Salgueiriño-Maceira, V.; Correa-Duarte, M.; Farle, M.; López-Quintela, A.; Sieradzki, K.; Diaz, R. *Chem. Mater.* **2006**, *18*, 2701–2706. (l) Choi, J. s.; Jun, Y.-w.; Yeon, S.-I.; Kim, H. C.; Shin, J.-S.; Cheon, J. *J. Am. Chem. Soc.* **2006**, *128*, 15982–15983. (m) Lee, J.-H.; Jun, Y.-w.; Yeon, S.-I.; Shin, J.-S.; Cheon, J. *Angew. Chem., Int. Ed.* **2006**, *45*, 8160–8162. (n) Kwon, K.-W.; Lee, B. H.; Shim, M. *Chem. Mater.* **2006**, *18*, 6357–6363. (o) Pellegrino, T.; Fiore, A.; Carlino, E.; Giannini, C.; Cozzoli, P. D.; Ciccarella, G.; Respaud, M.; Palmirotta, L.; Cingolani, R.; Manna, L. *J. Am. Chem. Soc.* **2006**, *128*, 6690–6698. (p) Casavola, M.; Grillo, V.; Carlino, E.; Giannini, C.; Gozzo, F.; Pinel, E. F.; Garcia, M. A.; Manna, L.; Cingolani, R.; Cozzoli, P. D. *Nano Lett.* **2007**, *7*, 1386–1395. (q) Salant, A.; Amitay-Sadovsky, E.; Banin, U. *J. Am. Chem. Soc.* **2006**, *128*, 10006–10007. (r) Petruska, M. A.; Bartko, A. P.; Klimov, V. I. *J. Am. Chem. Soc.* **2004**, *126*, 714–715. (s) Teranishi, T.; Saruyama, M.; Nakaya, M.; Kanehara, M. *Angew. Chem., Int. Ed.* **2007**, *46*, 1713–1715. (t) Tada, H.; Mitsui, T.; Kiyonaga, T.; Akita, T.; Tanaka, K. *Nat. Mater.* **2006**, *5*, 782–786. (u) Choi, S.-H.; Kim, E.-G.; Hyeon, T. *J. Am. Chem. Soc.* **2006**, *128*, 2520–2521. (v) Habas, S. E.; Yang, P.; Mokari, T. *J. Am. Chem. Soc.* **2008**, *130*, 3294–3295.

(8) (a) Yu, H.; Chen, M.; Rice, P. M.; Wang, S. X.; White, R. L.; Sun, S. *Nano Lett.* **2005**, *5*, 379–382. (b) Li, Y.; Zhang, Q.; Nurmikko, A. V.; Sun, S. *Nano Lett.* **2005**, *5*, 1689–1692. (c) Xu, C.; Xie, J.; Ho, D.; Wang, C.; Kohler, N.; Walsh, E. G.; Morgan, J. R.; Chin, Y. E.; Sun, S. *Angew. Chem., Int. Ed.* **2007**, *47*, 173–176.

Scheme 1. (a) Preparation of Two Kinds of Oligonucleotide-Conjugated Au−Fe_3O_4 Heterostructured Nanoparticles (P1−Au−Fe_3O_4 and P2−Au−Fe_3O_4) and (b) Their Detection of Complementary Oligonucleotides

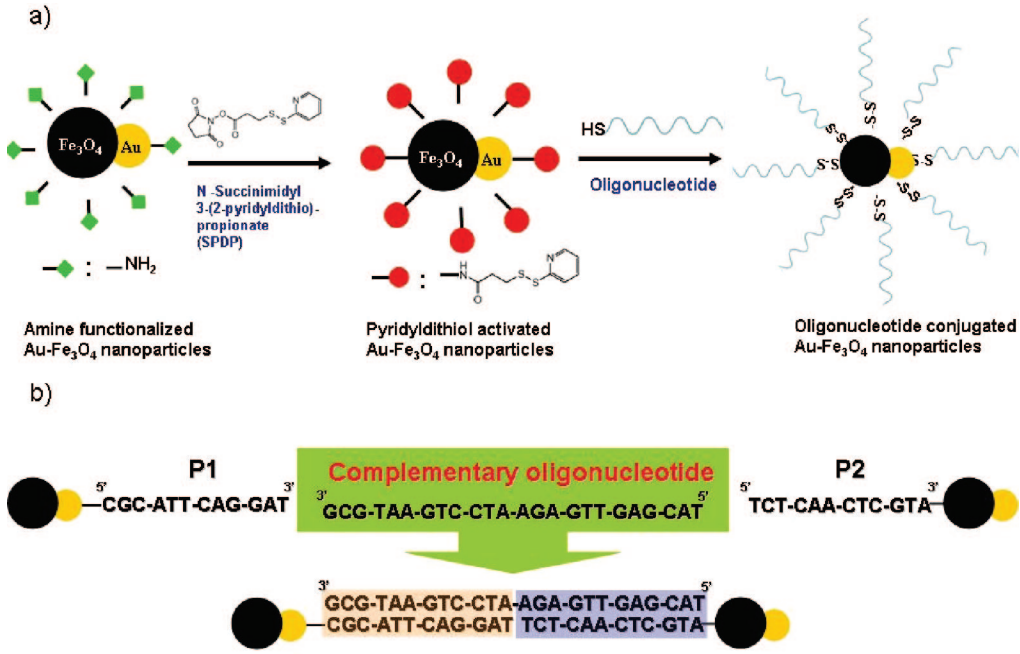

T_1)]M_0| using a nonlinear least-squares fit with the Levenberg−Marquardt algorithm.[10]

Oligonucleotide-Conjugated Au−Fe_3O_4 Heterostructured Nanoparticles. Scheme 1 summarizes the preparation of oligonucleotide-conjugated Au−Fe_3O_4 nanoparticles and their subsequent hybridization with complementary oligonucleotide sequences. Amino-functionalized Au−Fe_3O_4 nanoparticles were prepared by a procedure similar to that used for the water-dispersed Au−Fe_3O_4 nanoparticles. To attach amine groups to the surface of the nanoparticles, we used a mixture of 1,2-distearoyl-*sn*-glycero-3-phosphoethanolamine-*N*-[methoxy(polyethylene glycol)-2000] and 1,2-distearoyl-*sn*-glycero-3-phosphoethanolamine-*N*-[amino(polyethylene glycol)-2000] (Avanti Polar Lipids, Inc.) with a molar ratio of 5:1. A 0.5 mL sample of these nanoparticles (0.35 mg of Fe and 0.41 mg of Au) was mixed with 20 μL of *N*-succinimidyl 3-(2-pyridyldithio)propionate (SPDP) solution (20 mM in PBS). After 30 min, the resulting pyridyldithiol-activated nanoparticles were purified using a desalting column (Sephadex G-25).

The pyridyldithiol-activated nanoparticles were linked to two 12-base thiolated oligonucleotides [HS-CGC-ATT-CAG-GAT (P1) and TCT-CAA-CTC-GTA-SH (P2)] by forming disulfide bonds.[11] Each of the sequences P1 and P2 were chosen to recognize one of the two 12-base halves of the 24-mer DNA sequence GCG-TAA-GTC-CTA-AGA-GTT-GAG-CAT. For the conjugation of the two 12-base oligonucleotide sequences to the Au−Fe_3O_4 nanoparticles, 77 μL of oligonucleotide (7.7 nmol) was mixed with the SPDP-treated nanoparticles and incubated for 12 h at room temperature. After the separation of nonconjugated oligonucleotides using a 100 kDa membrane, the oligonucleotide-conjugated nanoparticles, designated as P1−Au−Fe_3O_4 and P2−Au−Fe_3O_4, were highly stable and kept dispersed in water for extended periods.

Detection of cDNA Sequences by Oligonucleotide-Conjugated Au−Fe_3O_4 Nanoparticles. To probe their ability to sense cDNA sequences, the two types of oligonucleotide-conjugated Au−Fe_3O_4 nanoparticles (P1−Au−Fe_3O_4 and P2−Au−Fe_3O_4) were reacted with the complementary 24-mer oligonucleotide sequence given above. Mixtures of P1−Au−Fe_3O_4 nanoparticles (100 μL) and P2−Au−Fe_3O_4 nanoparticles (100 μL) were incubated with 20 μL of the complementary oligonucleotide sequence, and the conjugation process was traced using three kinds of analytical tools: dynamic light scattering (DLS) to detect changes in the overall particle size, optical absorption spectroscopy to probe shifts in the absorption profile of the Au component, and MRI to evaluate changes in the relaxation effect of the Fe_3O_4 component.

Results and Discussion

Syntheses of uniform-sized nanoparticles via thermal decomposition of metal−surfactant complexes prepared from the reaction of inexpensive metal salts and surfactants have been previously reported.[9] For example, uniform-sized nanoparticles of Fe_3O_4,[9a] MnO,[9a] CoO,[9b] and ZnO[9c] were synthesized by thermal decomposition of the corresponding metal−oleate complexes, whereas uniform Pd nanoparticles[9d] were synthesized via thermolysis of a Pd−trioctylphosphine complex. The current heterostructured oxide−metal nanoparticles were synthesized via thermal decomposition of mixtures of metal−oleate (for Fe_3O_4 and MnO) and metal−oleylamine (for Au, Ag, Pt, and Ni) complexes.

TEM images of the synthesized Au−Fe_3O_4 heterostructured nanoparticles are shown in Figure 1a,b. The overall shape of the heterostructured nanoparticles was similar to a bent or triangular-pyramidal shape resembling that of a water or ammonia molecule, respectively, with a Au nanoparticle in the corresponding O or N position and Fe_3O_4 nanoparticles in the

(9) (a) Park, J.; An, K.; Hwang, Y.; Park, J.-G.; Noh, H.-J.; Kim, J.-Y.; Park, J.-H.; Hwang, N.-M.; Hyeon, T. *Nat. Mater.* **2004**, *3*, 891–895. (b) An, K.; Lee, N.; Park, J.; Kim, S. C.; Hwang, Y.; Park, J. G.; Kim, J. Y.; Park, J. H.; Han, M. J.; Yu, J.; Hyeon, T. *J. Am. Chem. Soc.* **2006**, *128*, 9753–9760. (c) Choi, S.-H.; Kim, E.-G.; Park, J.; An, K.; Lee, N.; Kim, S. C.; Hyeon, T. *J. Phys. Chem. B* **2005**, *109*, 14792–14794. (d) Kim, S.-W.; Park, J.; Jang, Y.; Chung, Y.; Hwang, S.; Hyeon, T.; Kim, Y. W. *Nano Lett.* **2003**, *3*, 1289–1291. (e) Bao, N.; Shen, L.; Wang, Y.; Padhan, P.; Gupta, A. *J. Am. Chem. Soc.* **2007**, *129*, 12374–12375. (f) Yu, W. W.; Falkner, J. C.; Yavuz, C. T.; Colvin, V. L. *Chem. Commun.* **2004**, 2306–2307. (g) Jana, N. R.; Chen, Y.; Peng, X. *Chem. Mater.* **2004**, *16*, 3931–3935.
(10) Zhu, D. C.; Penn, R. D. *Magn. Reson. Med.* **2005**, *54*, 725–731.
(11) (a) Perez, J. M.; Josephson, L.; O'Loughlin, T.; Högemann, D.; Weissleder, R. *Nat. Biotechnol.* **2002**, *20*, 816–820. (b) Josephson, L.; Perez, J. M.; Weissleder, R. *Angew. Chem., Int. Ed.* **2001**, *40*, 3204–3206.

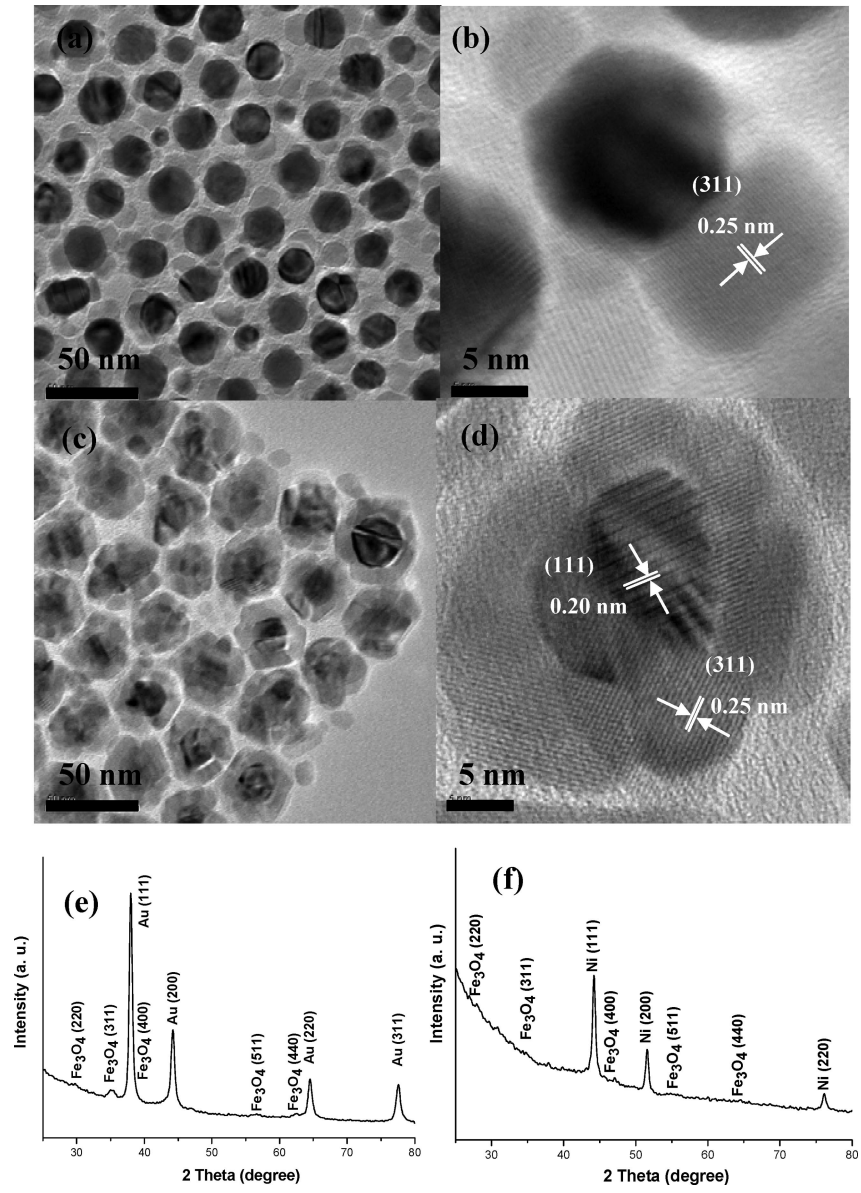

Figure 1. TEM and HRTEM images and XRD patterns of (a, b, e) Au−Fe_3O_4 heterostructured nanoparticles and (c, d, f) Ni−Fe_3O_4 heterostructured nanoparticles.

H positions. The mean size of the Au−Fe_3O_4 nanoparticles was ~33 nm with spherical Au components of 22 nm. The high-resolution TEM (HRTEM) image clearly shows the (311) planes of the Fe_3O_4 component with a *d*-spacing of 0.25 nm. The XRD pattern (Figure 1e) revealed that these nanoparticles were composed of face-centered cubic (fcc)-structured Fe_3O_4 (JCPDS No. 88-0315) and fcc-structured Au (JCPDS No. 04-0784).

The Ni−Fe_3O_4 heterostructured nanoparticles, which were synthesized via a very similar procedure, had a flowerlike shape, with the Fe_3O_4 components as petals and the Ni components as pistils. The TEM image (Figure 1c) showed that the mean size of the Ni−Fe_3O_4 nanoparticles was ~42 nm with spherical Ni components of 22 nm. The (111) planes of a Ni component, with a *d*-spacing of 0.20 nm, and the (311) planes of an Fe_3O_4 component are clearly shown in the HRTEM image (Figure 1d). The XRD pattern (Figure 1f) showed that these nanoparticles were composed of fcc-structured Fe_3O_4 and fcc-structured nickel (JCPDS No. 87-0712).

Heterostructured nanoparticles of Ag−MnO and Au−MnO had an overall shape that was snowmanlike, with the metal component in the top part and the MnO component in the bottom part. According to the TEM image (Figure 2a), the mean size of the Ag−MnO nanoparticles was 21 nm and that of the Ag component was 9 nm. The HRTEM image (Figure 2b) shows the (200) planes of the MnO component with a *d*-spacing of 0.22 nm. The mean size of the Au−MnO nanoparticles was ~32 nm and that of the Au component was 8 nm. The energy dispersive X-ray spectroscopy (EDS) data showed that the nanoparticles are composed of Au and Mn species (Figure S1b in the Supporting Information). The snowmanlike shape of the Au−MnO nanoparticles was confirmed by changing the tilt angle ($X°$, $Y°$) during the TEM measurement (Figure S2 in the Supporting Information); the resulting series of images showed a gradual change from a core/shell-like structure to the snowmanlike structure. The XRD patterns of the heterostructured nanoparticles of Ag−MnO (Figure 2e) and Au−MnO (Figure 2f) showed that they were composed of fcc-MnO (JCPDS 07-0230 or 78-0424) and either fcc-Ag (JCPDS No. 87-0720) or fcc-Au (JCPDS No. 04-0784).

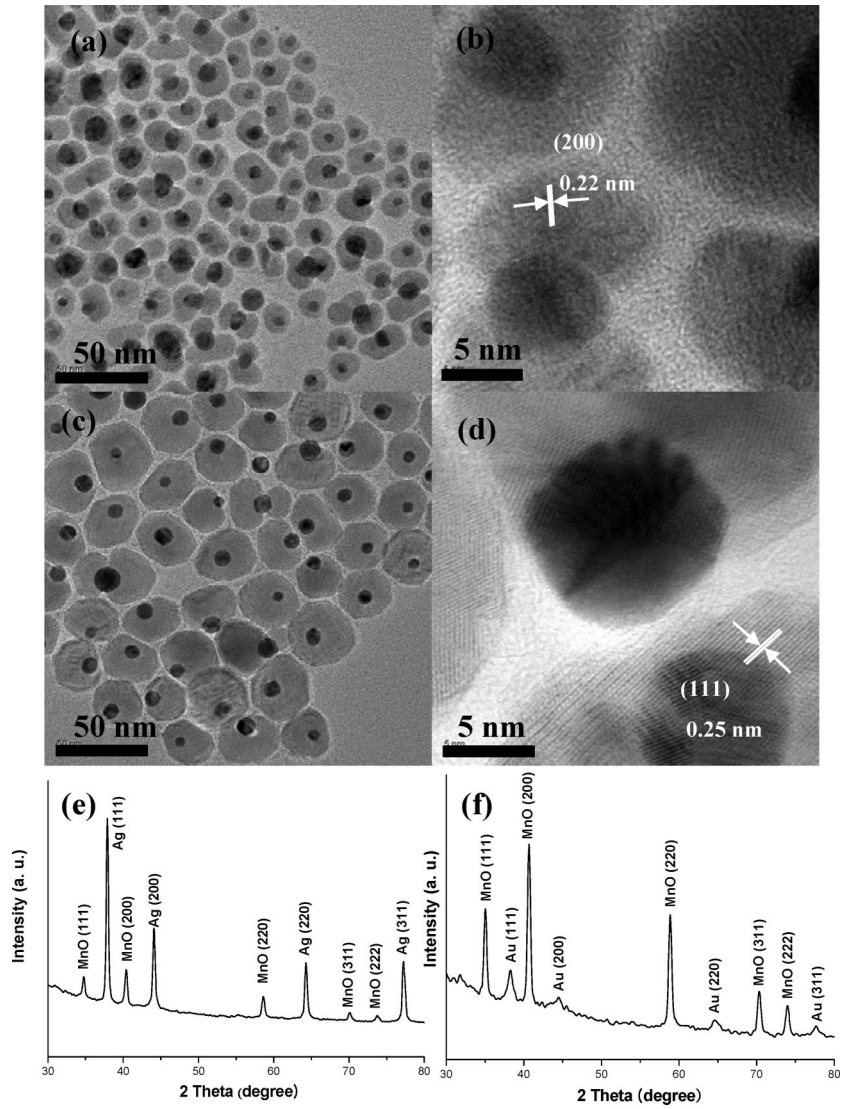

Figure 2. TEM and HRTEM images and XRD patterns of (a, b, e) Ag−MnO heterostructured nanoparticles and (c, d, f) Au−MnO heterostructured nanoparticles.

To understand the formation mechanism of the heterostructured nanoparticles, we conducted sampling experiments by collecting aliquots at various stages during the synthesis of the Au−MnO nanoparticles and analyzing them with TEM (Figure S3 in the Supporting Information). When the reaction mixture, composed of Au−oleylamine complex solution either alone or mixed with Mn−oleate complex, was heated to 140 °C, Au nanoparticle seeds were generated. The TEM image taken after heating the reaction mixture composed of Au−oleylamine complex and Mn−oleate complex to 280 °C revealed that only Au nanoparticles were generated and no heterostructured nanoparticles had yet been produced. However, when the reaction mixture was heated to 300 °C, we can clearly observe the formation of the heterostructured Au−MnO nanoparticles. In summary, we propose the following formation mechanism for the heterostructured Au−MnO nanoparticles. At first, gold nanoparticle seeds are generated from the reduction of the gold salt by oleylamine,[7b,12] probably with an assist from sonication. At 300 °C, the MnO part, which was generated from the thermal decomposition of the Mn−oleate complex, grows on the Au nanoparticle seeds via a seed-mediated growth process, producing the heterostructured Au−MnO nanoparticles.

Thermal decomposition of the mixture of Fe−oleate and Pt−oleylamine complexes also produced flowerlike-shaped Pt−Fe_3O_4 heterostructured nanoparticles, with Fe_3O_4 nanoparticles as petals and Pt nanoparticles as pistils. TEM images (Figure 3a,b) revealed that the mean size of the nanoparticles was 64 nm and that of the aggregated Pt component was 24 nm. The HRTEM image (Figure 3c) shows the (311) planes of the Fe_3O_4 nanoparticles, and the ED and XRD patterns (Figure 3d,e) showed that the nanoparticles were composed of fcc-Fe_3O_4 and fcc-Pt (JCPDS No. 87-0646). The EDS data showed that the nanoparticles were composed of Fe and Pt species (Figure S1a in the Supporting Information). Magnetization curves (Figure S4 in the Supporting Information) showed that these Pt−Fe_3O_4 nanoparticles were weakly ferromagnetic with a very small coercive field at 5 K but became superparamagnetic at 300 K.

The combination of different nanostructured materials will allow the development of novel multifunctional nanomedical platforms for multimodal imaging or simultaneous diagnosis and therapy.[13] Superparamagnetic iron oxide (SPIO) has been extensively used as a T_2 MRI contrast agent, and more recently, our group developed a T_1 MRI contrast agent based on MnO

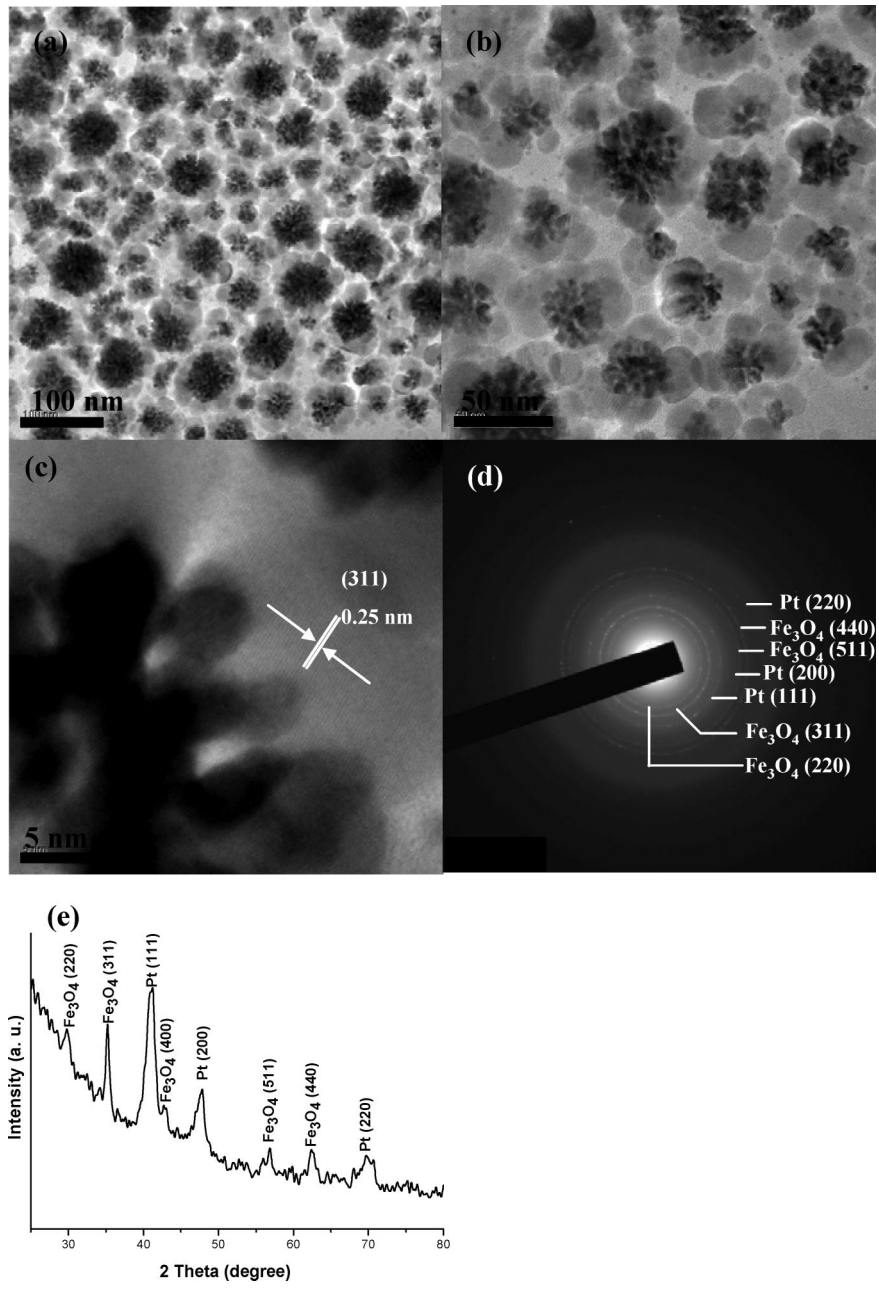

Figure 3. (a, b) TEM images, (c) HRTEM image, (d) ED pattern and (e) XRD pattern of flowerlike Pt−Fe_3O_4 heterostructured nanoparticles.

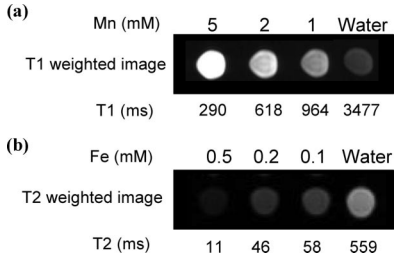

Figure 4. (a) T_1-weighted images and relaxation times at various concentrations of Au−MnO heterostructured nanoparticles. (b) T_2-weighted images and relaxation times at various concentrations of Au−Fe_3O_4 heterostructured nanoparticles.

nanoparticles.[4] Weissleder and co-workers[11a] developed biocompatible magnetic relaxation switches for detecting molecular interactions, such as DNA−DNA, protein−protein, protein−small-molecule, and enzyme reactions, based on the observation that self-assembled magnetic nanoparticles exhibit enhanced spin−spin relaxation (T_2 relaxation) compared to that of the individual magnetic nanoparticles. On the other hand, oligonucleotide-modified Au nanoparticles assemble sequence-specifically with complementary target DNA and induce changes in the particle−particle surface plasmon interactions and aggregate scattering properties, enabling a colorimetric assay of the degree of hybridization of DNA strands.[14] Furthermore, the melting profiles of the Au nanoparticle-labeled DNA aggregates were extraordinarily sharp. Utilizing these interesting characteristics of the oligonucleotide-modified Au nanoparticles, Mirkin and co-workers[15] were able to differentiate DNA with single base-pair mismatches simply by measuring absorbance as a function of temperature.

On the basis of these previous biomedical applications of nanoparticles of Au, Fe_3O_4, and MnO, the current synthesized heterostructured nanoparticles of Au−MnO and Au−Fe_3O_4 have

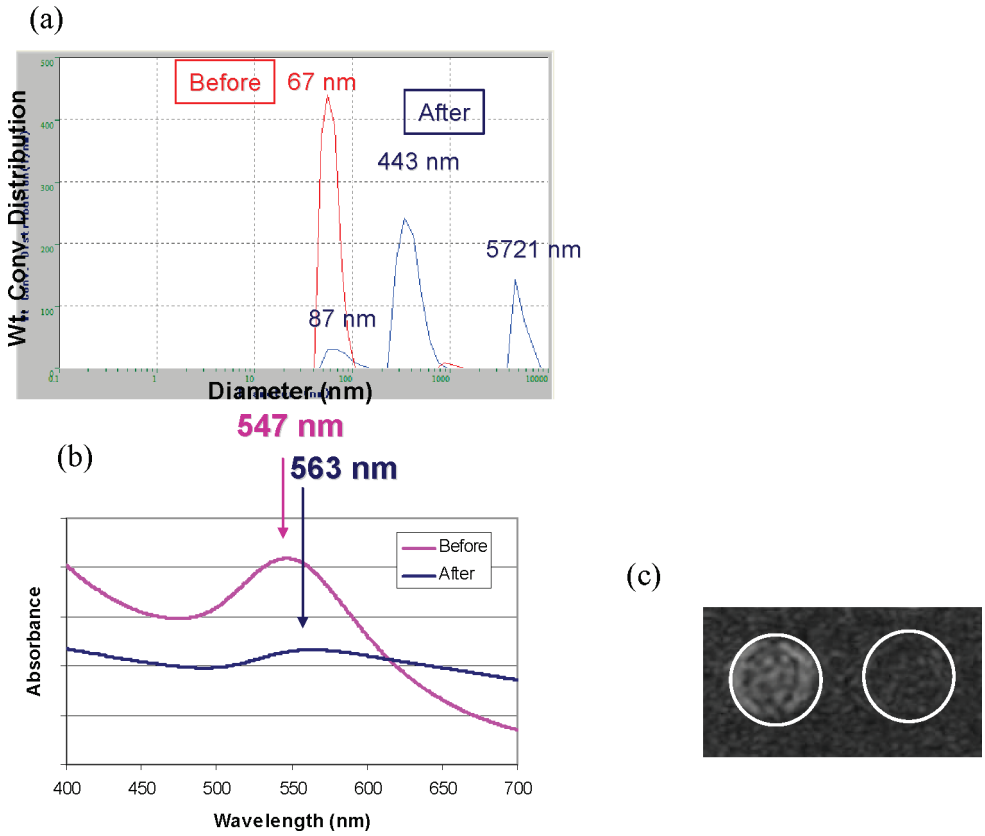

Figure 5. Probing the sensing of cDNA sequences by the two types of oligonucleotide-conjugated Au−Fe_3O_4 nanoparticles: (a) change of size by dynamic light scattering; (b) change of absorption profile; (c) change of contrast in T_2-weighted MRI.

great potential to be used for multimodal biomedical probes. First, we prepared water-dispersed nanoparticles of Au−MnO and Au−Fe_3O_4 by encapsulating the nanoparticles with a PEG−phospholipid shell.[5a] DLS data showed that the dispersed Au−MnO and Au−Fe_3O_4 nanoparticles were highly stable and did not aggregate and that the hydrodynamic diameters were 44 and 42 nm, respectively (Figure S5 in the Supporting Information). To examine the possibility of using these nanoparticles as MRI contrast agents, the relaxation times of the nanoparticles prepared in test tubes were measured with a 1.5 T human clinical scanner. Figure 4a,b shows the T_1- and T_2-weighted images and their relaxation times for different concentrations of Au−MnO and Au−Fe_3O_4 nanoparticles, respectively. In a further investigation of their contrast effects, measurement of the specific relaxivities (r_1 and r_2) revealed that the Au−MnO nanoparticles had an r_1 of 0.6 mM^{-1} s^{-1} and an r_2 of 1.8 mM^{-1} s^{-1} whereas the Au−Fe_3O_4 nanoparticles had an r_1 of 4.6 mM^{-1} s^{-1} and an r_2 of 204 mM^{-1} s^{-1}. These values are similar to those of previously reported nanoparticles of MnO and Fe_3O_4,[3,4] demonstrating that these heterostructured nanoparticles are suitable candidates for MRI contrast agents.

Au−Fe_3O_4 heterostructured nanoparticles have the potential to serve as bimodal sensors for detecting cDNA sequences because their self-assembly causes the changes in the absorption spectrum and the T_2 contrast effect as described above. As a model experiment, the two 12-base oligonucleotides P1 and P2 were linked to Au−Fe_3O_4 nanoparticles, yielding nanoparticles labeled as P1−Au−Fe_3O_4 and P2−Au−Fe_3O_4, respectively; these were allowed to hybridize to a single-stranded DNA that was complementary to both P1 and P2. The DLS data showed that the mean hydrodynamic radius increased upon incubation of the mixture of oligonucleotide-linked nanoparticles and cDNA strands, confirming the hybridization with the complementary oligonucleotides (Figure 5a). The optical absorption spectra (Figure 5b) revealed the red shift of the surface plasmon resonance band from 547 to 563 nm, and the signal intensity of the T_2-weighted MRI image (Figure 5c) was significantly enhanced via the hybridization process, confirming the aggregation of the nanoparticles. These results clearly demonstrate that these nanoparticles can be used as multimodal detection or imaging probes for various biomedical applications.

Conclusion

In conclusion, heterostructured nanoparticles composed of various combinations of a metal (Au, Ag, Pt, or Ni) and an oxide (Fe_3O_4 or MnO) can be readily synthesized from thermal decomposition of mixtures of metal−oleate complexes and metal−oleylamine complexes. The current synthetic procedure is very simple and highly reproducible. Furthermore, nanoparticles of Au−MnO and Au−Fe_3O_4 have the potential to serve in many multifunctional biomedical applications, such as multimodal imaging or detection probes. We expect that the current simple synthetic method can be extended to the synthesis of many other heterostructured nanoparticles. Furthermore, these heterostructured nanoparticles will find many multifunctional biomedical applications, such as multimodal detection or imaging probes.

(12) Lu, X.; Yavuz, M.; Tuan, H.-Y.; Korgel, B. A.; Xia, Y. *J. Am. Chem. Soc.* **2008**, *130*, 8900–8901.
(13) Kim, J.; Piao, Y.; Hyeon, T. *Chem. Soc. Rev.* **2008**, in press; DOI: 10.1039/B709883A.
(14) Storhoff, J. J.; Mirkin, C. A. *Chem. Rev.* **1999**, *99*, 1849–1862.

Acknowledgment. We thank the Korean Ministry of Education, Science and Technology for funding through the National Creative Research Initiative Program of the Korea Science and Engineering Foundation (KOSEF). We thank Yong Sik Bang of Seoul National University Hospital for help with the MRI measurements.

(15) (a) Mirkin, C. A.; Letsinger, R. L.; Mucic, R. C.; Storhoff, J. J. *Nature* **1996**, *382*, 607–609. (b) Rosi, N. L.; Mirkin, C. A. *Chem. Rev.* **2005**, *105*, 1547–1562. (c) Storhoff, J. J.; Lazarides, A. A.; Mirkin, C. A.; Letsinger, R. L.; Mucic, R. C.; Schatz, G. C. *J. Am. Chem. Soc.* **2000**, *122*, 4640–4650.

Supporting Information Available: EDS data for Pt−Fe_3O_4 and Au−MnO nanoparticles, ($X°$, $Y°$)-tilted TEM images of Au−MnO nanoparticles, TEM images of the aliquots collected during the synthesis of Au−MnO nanoparticles, hysteresis curves measured at 5 and 300 K for the Pt−Fe_3O_4 heterostructured nanoparticles, and hydrodynamic diameter distributions for water-dispersed Au−MnO and Au−Fe_3O_4 heterostructured nanoparticles. This material is available free of charge via the Internet at http://pubs.acs.org.

JA805311X